IWLHS, 20-22/02/2013, Aachen - Bung & Pagliara (eds) - © 2013 Bundesanstalt für Wasserbau ISBN 978-3-939230-04-5

Air Entrainment and Energy Dissipation on Porous Pooled Stepped Spillways

S. Felder & H. Chanson
The University of Queensland, School of Civil Engineering, Brisbane QLD 4072, Australia

ABSTRACT: The hydraulics of stepped spillways with flat steps is well documented and some design guidelines exist for typical embankment dam slopes. On the other hand, alternative stepped designs are poorly understood. In the present study, some porous pooled stepped spillways were investigated with two different porosities of the pooled weir. The air-water flow patterns, air-water flow properties and the energy dissipation rate were observed and compared to the corresponding flat and pooled stepped spillways. The comparative study highlighted a larger interfacial velocity for the pooled step configurations. The largest residual energy at the downstream end was observed for the porous pooled steps which was associated with reduced cavity recirculation and form drag. Overall the porous pooled stepped design exhibited some more stable flow patterns than the pooled stepped design, but it was characterised by a lesser rate of energy dissipation than the flat step design for the investigated slope (θ = 26.6°).

Keywords: Stepped spillways, Porous pooled steps, Pooled steps, Flow aeration, Energy dissipation, Flow resistance, Drag reduction

1 INTRODUCTION

Stepped spillways are an advantageous design for flood release facilities on embankment dam stepped spillways and low head hydraulic structures. The steps act as large rough elements increasing the air entrainment and energy dissipation performances compared to smooth chutes (Chanson 2001). The stepped spillway design is compatible with modern construction techniques including roller compacted concrete (RCC) and gabions. Further its selection reduces the cavitation risk and no damage has been reported. The stepped spillway design is often designed for skimming flows, and the aeration and energy dissipation performances are well documented for flat uniform stepped spillways with embankment dam slopes (Chanson 2001, Ohtsu et al. 2004, Gonzalez & Chanson 2007, Felder & Chanson 2009, Bung 2011).

The stepped spillway design is not limited to flat uniform steps and some prototype stepped chutes were designed with non-uniform steps (e.g. Tillot dam, France), downwards inclined steps (e.g. Brushes Clough Dam, UK), changing channel slope (e.g. New Victoria dam, Australia), pooled steps (e.g. Sorpe dam, Germany) and weir structures designed with gabion steps. An optimum design in terms of energy dissipation and air entrainment might not be known yet. Some studies provided some insights into some more complex dam designs (e.g. Gonzalez & Chanson 2008, Relvas & Pinheiro 2008, Felder & Chanson 2011). Peyras et al. (1992) studied the energy dissipation over gabion stepped weirs. In recent years, the air-water flows on pooled stepped spillways were researched with channel slopes of 14.6°, 18.6° and 30° (André 2004, Kökpinar 2004, Thorwarth & Köngeter 2006). Some self-induced instabilities on a pooled stepped spillway with θ = 8.9° were investigated in detail by Thorwarth (2008) and Felder & Chanson (2012). The instabilities comprised jump waves which traveled downstream and might cause a risk for safe discharge of the stepped chute.

In the present study, some further pooled step designs were tested for a stepped spillway with θ = 26.6° comprising flat, pooled and porous pooled stepped configurations with porosities Po = 5% and Po = 31%. The investigations aimed to provide some insights on the flow patterns, as well as the aeration and energy dissipation performances for the (porous) pooled step designs.

2 EXPERIMENTAL CONFIGURATIONS AND INSTRUMENTATION

2.1 *Experimental facility and phase detection intrusive probes*

The experimental study was conducted in a large size stepped spillway facility with a 7 m long, 0.52 m wide test section with a slope of 26.6°. The channel consisted of 10 plywood steps with step height h = 10 cm and perspex sidewalls for flow visualization. Constant flow rates were supplied by a large upstream intake basin which supplied smooth waveless inflow into the test section through a long sidewall convergent with a 4.23:1 contraction ratio. At the upstream end of the test section, the flow was controlled by a broad-crested weir with height of 1 m, width W = 0.52 m and length L_{crest} = 1.01 m and an upstream rounded corner (r_{crest} = 0.08 m).

The air-water flow experiments were conducted with a double-tip conductivity probe (inner diameter $Ø$ = 0.25 mm). The leading and trailing tips of the probe were offset in longitudinal direction Δx = 7.2 mm with a transverse separation of Δz = 2.1 mm. The probe was supported by a trolley system and the positioning of the probes normal to the pseudo-bottom was performed with a Mitutoyo™ digital ruler mounted on a fine adjustment screw-drive mechanism. The error in the translation of the probe in the direction normal to the flow was less than 0.5 mm. The accuracy on the longitudinal probe position was estimated as Δx < +/- 0.5 cm. All measurements were conducted with an electronic system (Ref. UQ82.518) and the signal was acquired with a high speed data acquisition system (NI USB-6251) and a self-designed LabVIEW™ data acquisition software. In a detailed sensitivity analysis, a sampling duration of 45 s and a sampling rate of 20 kHz were identified as optimum for the accurate recording of the air-water flow properties. More details about the stepped spillway facility were reported by Felder et al. (2012).

2.2 *Experimental configurations*

The experiments encompassed four uniform stepped spillway configurations, i.e. flat steps, pooled steps and porous pooled steps with Po = 5% and Po = 31% (Figure 1). The pool weir height for all pooled configurations was w = 3.1 cm. The pores on the porous pooled steps had a diameter $Ø$ = 5 mm and were distributed evenly on the pooled weir (Figure 2). Detailed visual observations of the flow patterns were conducted for all step configurations for a range of discharges per unit widths $0.003 \leq q_w \leq 0.282$ m²/s. Some air-water flow measurements were performed with the double-tip conductivity probe downstream of the inception point of air entrainment for $0.025 \leq q_w \leq 0.250$ m²/s. The main focus of the investigations was the porous pooled design and the flat and pooled step designs were used as reference configurations.

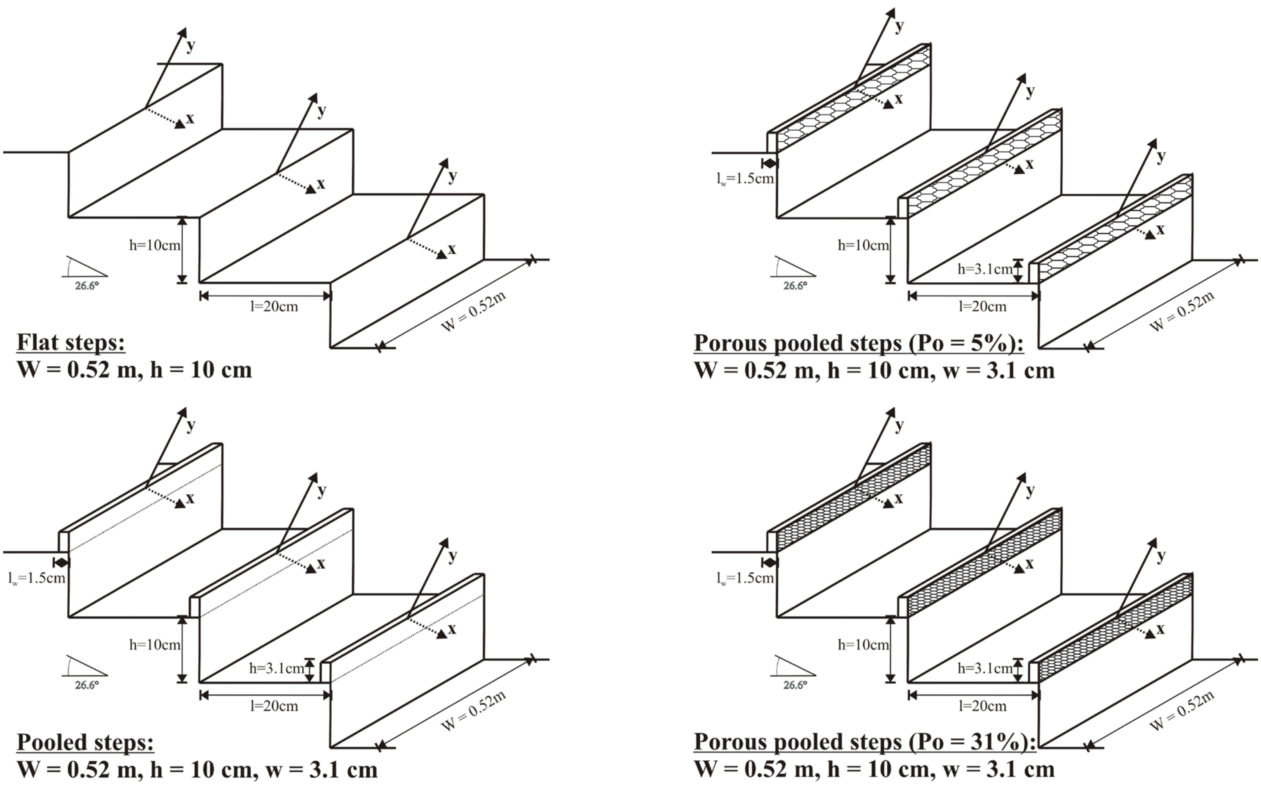

Figure 1. Detail of stepped spillway configurations with flat, pooled and porous pooled steps (θ = 26.6°); definition of first measurement position on flat and (porous) pooled steps (y = 0)

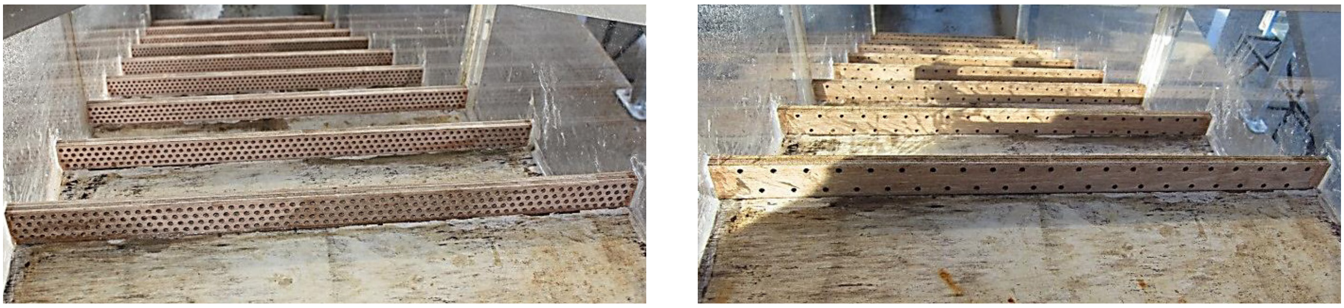

Figure 2. Photos of porous pooled stepped spillways with Po = 31% (Left) and Po = 5% (Right); Diameter of holes $Ø$ = 5 mm

3 AIR-WATER FLOW PATTERNS

The air-water flow patterns on the flat and pooled stepped spillways exhibited some typical features with nappe, transition and skimming flow regimes clearly distinguishable with increasing discharge. The changes in flow regimes were in good agreement and compared well with previous studies on embankment dams (Felder & Chanson 2009). For the pooled stepped spillway, some small instabilities were observed within the nappe flow regime for dimensionless flow rates $0.3 < d_c/h < 0.45$ with d_c the critical flow depth. The instabilities resulted from a pulsating flow within the first step cavity which caused some small deviations of the free-falling nappes. The flow disturbances were much smaller compared to the observations of Thorwarth (2008) and Felder & Chanson (2012) on a pooled stepped spillway with $\theta = 8.9°$ and same ratio of pool weir height to step length ($w/l = 0.155$). For $d_c/h \geq 0.45$, no instabilities were observed. Some more details about the instabilities and the flow patterns on the flat and pooled stepped spillways can be found in Felder et al. (2012). The change from transition to skimming flow was observed for $d_c/h = 0.9$ on the pooled stepped spillway and for $d_c/h = 0.97$ on the flat steps.

The air-water flow patterns on the porous pooled stepped spillways with Po = 5% and Po = 31% respectively exhibited typical nappe, transition and skimming flow regimes. The observations were in good agreement with the observations on the pooled stepped spillway, but for all flow rates, some differences were caused by some small discharges through the pores in the pooled weirs. Some estimates of the discharge through the pores were conducted for the different flow rates using classical resistance coefficients (Idelchik 1994). The discharge through the pores was estimated based upon the energy equation between either sides of the porous pooled wall:

$$\Delta H = \frac{\zeta \times U_{Po}^{2}}{2 \times g} \quad (1)$$

where ΔH is the energy difference between the two sides of the porous wall (herein the difference in free-surface elevation between one pool weir height upstream and downstream of the pool wall, identified using visual observations), ζ is the resistance coefficient for an perforated thick plate (Idelchik 1994), g is the gravity acceleration constant and U_{Po} is the stream wise velocity of the discharge through the pores. The maximum discharges through the pores based upon stationary flow considerations were estimated at less than 7% of the total flow discharge for the porous configuration Po = 31% and much less than 1% for Po = 5%. The discharges for the transition and nappe flows were comparatively larger because the downstream side of the pooled weir was not submerged and a void existed. Note that the discharge calculation through the pores was a rough estimate and the recirculations within the cavity, the irregular cavity ejections, and the non-horizontal angle between flow and pool weir might affect the porous flow estimate.

For the smallest flow rates d_c/h < 0.43-0.46, a nappe flow regime was observed for both porous pooled configurations. The flow pattern was similar to the nappe flows on the pooled stepped spillway, but some flow occured also through the pores. Importantly, for the nappe flow regime on both porous pooled stepped spillways, no pulsations were observed in the first pooled cavity and no instabilities were present. The pores tended to balance the pressure between adjacent pooled cavities and increased the stability of the nappe flows. The transition flow regime showed some instable flow patterns which were similar to observations of transition flows on the flat and pooled stepped spillways (Figure 3). In Figure 3, a typical transition flow regime is shown for the porous steps with Po = 5% indicating a small air-water flow jet at the second pooled weir edge and some small instabilities and strong droplet splashing downstream. With increasing discharge, the instabilities decreased. With the disappearance of the jet at the second pooled step weir, the flow became stable in the skimming flow regime. The transition flow regime for the porous pooled stepped spillway with Po = 31% was observed for $0.43 < d_c/h < 0.75$ and for Po = 5% for $0.46 < d_c/h < 0.91$. The larger porosity reduced the instable transition flow rates and provided more stable skimming flow conditions compared to the flat and pooled step configurations. The skimming flow regime was observed for $d_c/h > 0.75$ (Po = 31%) and $d_c/h > 0.91$ (Po = 5%) respectively. The flow patterns were very similar to typical skimming flows on the corresponding flat and pooled stepped spillways (Figure 4). The flow appeared very regular and some stable cavity recirculations were observed downstream of the inception point. Figure 4 highlights some details of the cavity processes and the air-water flows through the pores. It seemed that the cavity recirculations decreased with increasing porosity. Furthermore, the amount of air in the cavity appeared smaller for the porous pooled steps which indicated a smaller interaction between cavity and main stream flow and a lower air entrainment into the step niche. The flow through the pores decreased the size of the upward jet at the downstream end of the cavity compared to the pooled steps. The visual observations indicated that the pores affected the air-water cavity flows, but the overlying main stream flow patterns were very close to the corresponding flows on the flat and pooled stepped spillways.

The visual observations indicated that the air-water flows in the step cavity were affected by the pore discharges. Some similarities were observed to flows behind porous fences which lead to a reduced recirculation behind the fence with increasing fence porosity (Tsuhahara et al. 2012). It is believed, that the injection of fluid into the cavity reduced the drag coefficient. The drag reduction behind ventilated bodies was shown by several researchers (e.g. Abdul-Khader & Rai 1980, Suryanarayana et al. 1993, Naudascher & Rockwell 1994). A reduction in drag in the porous pooled stepped experiments would lead to a reduced flow resistance, an increased main stream velocity and a reduced energy dissipation rate.

Figure 3. Transition flow regime on porous pooled stepped spillway (Po = 5%): $d_c/h = 0.51$; $q_w = 0.036$ m^2/s; Re = 1.4×10^5

Figure 4. Cavity detail and flow through pores in skimming flow regime on porous pooled stepped spillways – Left: Po = 5%, $d_c/h = 1.44$; $q_w = 0.171$ m^2/s; Re = 6.8×10^5; Right: Po = 31%, $d_c/h = 0.86$; $q_w = 0.079$ m^2/s; Re = 3.1×10^5

4 AIR-WATER FLOW PROPERTIES

The air-water flow measurements with the double-tip conductivity probe were conducted at all step edges downstream of the inception point on the channel centerline. For the flat steps, the first vertical position of the probe was at the step edge (y = 0) and for the pooled steps at the pool weir edge (y = 0). For all air-water flow properties, the graphs comprised dimensionless distributions as functions of the dimensionless distance from the pseudo-bottom formed by the step edges and pooled weir edges respectively (Figures 5-7). On the left hand side of the figures, the air-water flow properties are shown as a function of y/Y_{90}, where Y_{90} is the characteristic air-water flow depth where the void fraction C = 90%. On the right hand side, the data are presented as a function of $(y + w)/d_c$ to highlight the effects of the pool weir upon the flow depth.

Some typical void fraction distributions are illustrated in Figure 5 for all stepped configurations showing some typical S-shapes which were observed in many previous studies on flat stepped spillways in transition and skimming flows (e.g. Chanson & Toombes 2002, Bung 2011). Little difference was visible between flat, pooled and porous pooled stepped spillways illustrated as functions of y/Y_{90}. The distributions of void fraction C matched well the advective diffusion equation of Chanson & Toombes (2002):

$$C = 1 - \tanh^2\left(K' - \frac{y/Y_{90}}{2\times D_o} + \frac{\left(y/Y_{90} - 1/3\right)^3}{3\times D_o}\right) \qquad (2)$$

where K' is an integration constant and D_o is a function of the mean air concentration C_{mean} only:

$$K' = 0.32745 + 1/2\times D_o - 8/81\times D_o \qquad (3)$$

$$C_{mean} = 0.762\times(1.0434 - \exp(-3.614\times D_o)) \qquad (4)$$

The mean air-concentration C_{mean} characterized the depth-average air content in terms of Y_{90}: C_{mean} = 1-d/Y_{90} where d is the equivalent clear water flow depth:

$$d = \int_{y=0}^{y=Y_{90}} (1-C)\times dy \qquad (5)$$

For the graph showing the void fraction as function of $(y+w)/d_c$, the results showed also little difference between the data. However the void fraction profile for the pooled steps was shifted upward by w/d_c (Figure 5). The comparison of the (porous) pooled configurations showed a very good agreement between pooled and porous pooled configuration with Po = 5%. The void fraction distributions for the porous pooled stepped spillway with Po = 31% were slightly lower and indicated some small differences in terms of flow depth which seemed to be linked with some discharges through the pooled weir pores (Figure 5).

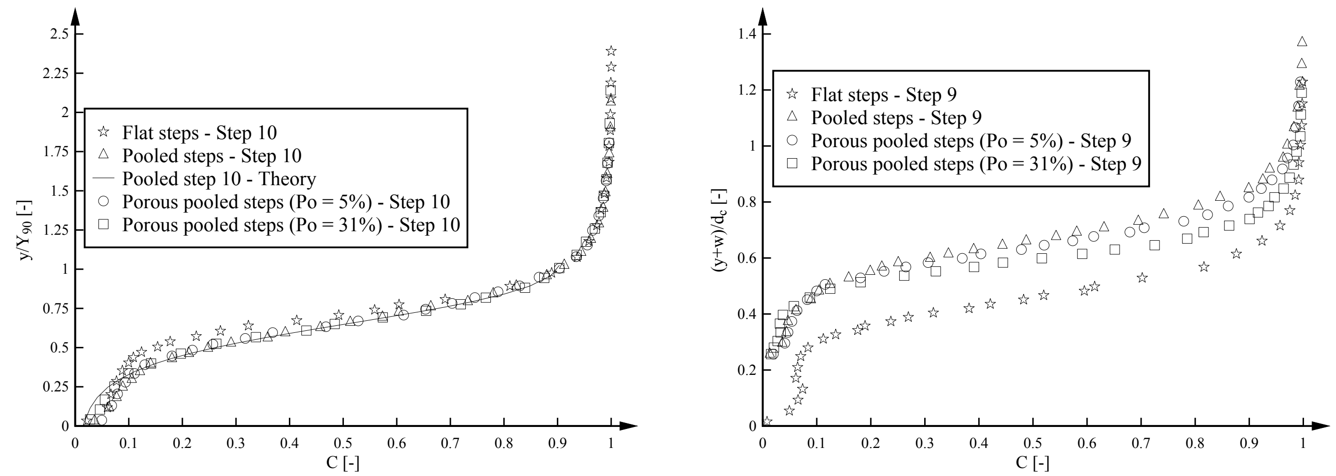

Figure 5. Comparison of void fraction distributions on the stepped spillways with flat, pooled and porous pooled steps – Left: d_c/h = 0.96; q_w = 0.094 m^2/s; Re = 3.7 × 10^5; Right: d_c/h = 1.29; q_w = 0.144 m^2/s; Re = 5.7 × 10^5; Comparison with advective diffusion equation (Equation (2))

The distributions of bubble count rate showed typical shapes with maxima in the intermediate flow region for void fractions of about C = 0.4 to 0.5 for all step configurations (Fig. 6). The number of entrained air bubbles was larger for the flat stepped spillway compared to the (porous) pooled step configurations. A close agreement in terms of bubble count rate distributions was observed for the pooled and porous pooled steps with Po = 5% for all discharges at all step edges. In contrast, a smaller bubble count rate was observed on the porous pooled stepped spillway with Po = 31%. The differences in bubble count rate between these configurations tended to decrease with increasing distance from the inception point of air entrainment. In Figure 6, some typical dimensionless distributions of bubble count rate $F \times d_c/V_c$ in transition and skimming flows are shown as functions of y/Y_{90} and $(y+w)/d_c$ where V_c the was the critical flow velocity. Note that, for all experiments, the equilibrium flow conditions were not achieved and the bubble count rate increased monotonically with longitudinal distance on all configurations and for all flow rates.

For all step configurations, some typical distributions of the dimensionless interfacial velocity V/V_{90} and V/V_c respectively are shown in Figure 7 as functions of y/Y_{90} and $(y+w)/d_c$. For the comparison of dimensionless interfacial velocity V/V_{90}, all data for the flat, pooled and porous pooled stepped spillways were in good agreement and they compared very well with some self-similar relationships:

$$\frac{V}{V_{90}} = \left(\frac{y}{y_{90}}\right)^{1/N} \qquad y/Y_{90} \leq 1 \quad (6)$$

$$\frac{V}{V_{90}} = 1 \qquad y/Y_{90} > 1 \quad (7)$$

For $y/Y_{90} \leq 1$, the data agreed well with a power law with exponent of N = 10 (Eq. (6), Figure 7). The exact value of N may vary from one step edge to the next one for a given flow rate. For $y/Y_{90} > 1$, the velocity distributions had a pseudo-uniform profile although some scatter of the data was observed in the spray region.

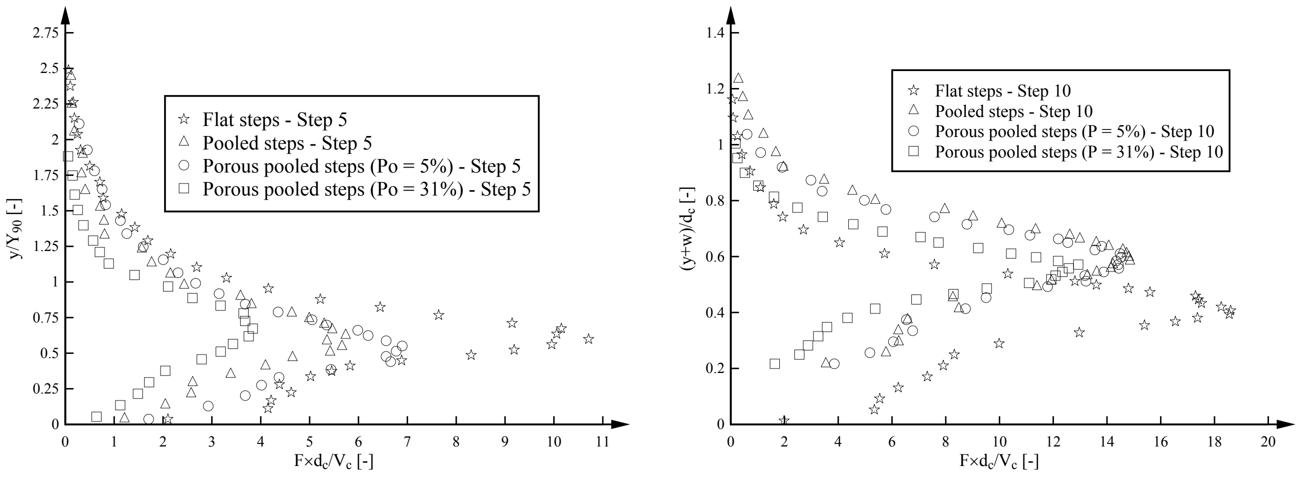

Figure 6. Comparison of bubble count rate distributions on the stepped spillways with flat, pooled and porous pooled steps – Left: d_c/h = 0.82; q_w = 0.073 m^2/s; Re = 2.9 × 10^5; Right: d_c/h = 1.52; q_w = 0.187 m^2/s; Re = 7.4 × 10^5

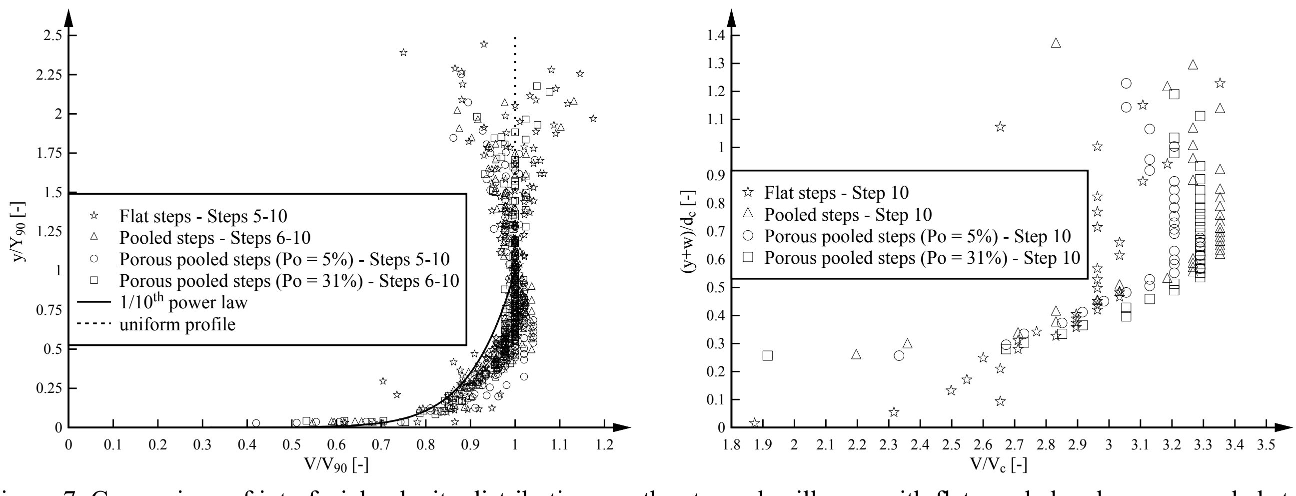

Figure 7. Comparison of interfacial velocity distributions on the stepped spillways with flat, pooled and porous pooled steps – Left: d_c/h = 0.96; q_w = 0.094 m^2/s; Re = 3.7 × 10^5; Right: d_c/h = 1.29; q_w = 0.144 m^2/s; Re = 5.7 × 10^5; Comparison with self-similar equations (Equations (6) & (7))

Some differences were however visible in terms of dimensionless interfacial velocity V/V_c (Fig. 7). For all present experiments, the data implied smaller interfacial velocities on the flat stepped spillway. This finding was counter-intuitive because it was assumed that the pooled steps increased the chute roughness and would slow down the spillway flows. Nonetheless, the present observations showed consistently a faster flow motion down the (porous) pooled stepped chutes for a wide range of discharges in transition and skimming flows. For all configurations, the interfacial velocities increased with increasing distance from the inception point. The interfacial velocities for the porous pooled step configurations were in between the flat and pooled stepped spillway velocities. The velocities for the porous pooled steps with Po = 31% and for the pooled steps were very close for all discharges with some slightly larger velocities for the pooled steps. The interfacial velocities tended to increase with increasing porosity and the data for the porous pooled steps with Po = 5% were consistently smaller compared to the steps with Po = 31%. The observations of the velocities for the (porous) pooled configurations did not follow a clear trend and the reason for the largest interfacial velocities on the pooled step configuration remained unclear. Overall the the interfacial velocity data $V_{\text{flat}} < V_{(\text{Po=5\%})} < V_{(\text{Po=31\%})} < V_{\text{pooled}}$ for a given flow rate and for all discharges.

5 ENERGY DISSIPATION AND FLOW RESISTANCE

5.1 *Residual energy*

For a design engineer, it is important to quantify the energy dissipation rate and the residual energy at the downstream end of stepped spillways. The rate of energy dissipation and the residual energy were calculated herein at the downstream end for the flat and (porous) pooled stepped spillway configurations. The calculations were based upon the air-water flow measurements with the double-tip conductivity probe. The residual head H_{res} at the location of measurement at the downstream end was:

$$H_{res} = d \times \cos\theta + \frac{U_w^{\ 2}}{2 \times g} + w \tag{8}$$

where U_w was the mean flow velocity $U_w = q_w/d$.

The observations of dimensionless residual head H_{res}/d_c at the last step edge or pool weir edge are illustrated in Figure 8 as a function of the dimensionless flow rate. Some differences in the residual head were observed for the different step configurations (8). The lowest residual head was achieved for the flat steps and the pooled steps exhibited a larger residual energy. This finding was surprising because it was expected that the pools would increase the energy dissipation along the pooled stepped chute as observed for flatter channel slopes (θ = 8.9°). The finding was consistent with the larger interfacial velocities on the pooled stepped spillway (Figure 7).

The largest residual energy was observed for the porous pooled stepped spillways with increasing residual head with increasing porosity. The larger residual energies for the porous pooled steps seemed to be linked with a reduced momentum exchange between the cavity and main stream flow caused by the pores in the pool weir. The pores in the pooled weir reduced both the energetic recirculation motions in the pooled step cavity and the form drag of the steps. Furthermore, some small discharge appeared through the pores and contributed to the reduced energy dissipation on the porous pooled stepped spillways. With increasing porosity, the energy dissipation performance decreased further.

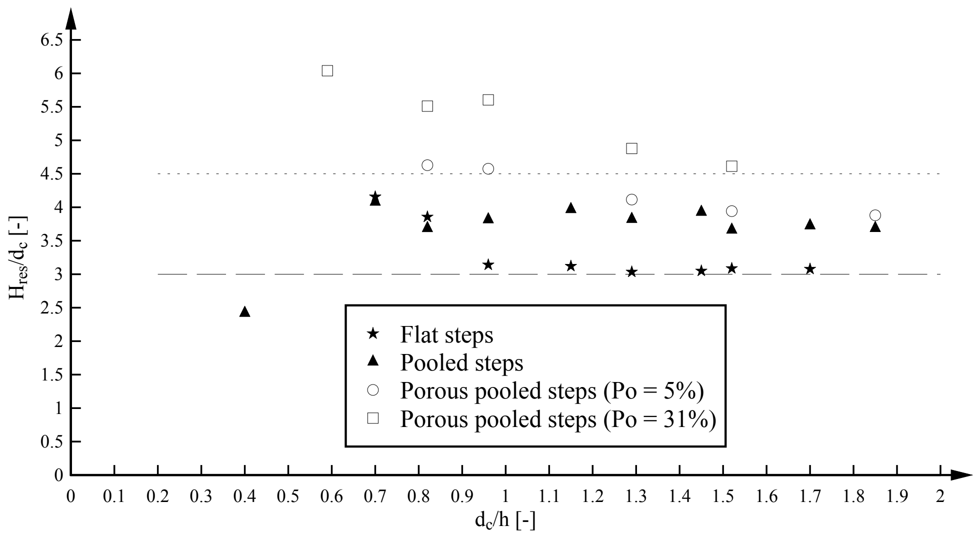

Figure 8. Comparison of dimensionless residual head at the downstream end on the stepped spillways with flat, pooled and porous pooled steps; Comparison with correlations of further stepped spillways with embankment dam slopes (dotted lines)

For all step configurations, the residual head decreased with increasing discharge for the smaller flow rates, while it was about constant for the largest flow rates. In Figure 8, the residual head data were compared with some simple design criteria for moderate slope-stepped spillways: the upper dotted line expressed the median residual energy of a number of experimental data obtained for flat stepped spillway slopes smaller than 15.9° and the lower dashed line the median values for flat stepped spillway data with slopes 21.8° < θ < 26.6° (Felder & Chanson 2009). Please note that the present flat stepped spillway data were not included in the median values. However, the present findings on the flat stepped spillway agreed very well with the previous physical studies on flat stepped spillways used for the median values shown in Figure 8. The residual energy for the (porous) pooled stepped spillways exceeded the correlations.

Note that, for the largest flow rates, the discharge was not fully developed at the downstream end of the spillway and the residual energy might be overestimated (Chanson 2001, Meireles & Matos 2009). The residual head at the downstream end of the stepped chute might be slightly larger than the specific energy at the start of the spillway apron. Hence, Figure 8 is suitable for design purposes including non-design flow conditions because it is conservative.

5.2 *Flow resistance*

On stepped spillways, some significant form losses are caused by the steps (Chanson 2001). Some additional flow resistance might be caused by the weir on pooled stepped spillways. The flow resistance is commonly expressed by the Darcy-Weisbach friction factor f_e (Rajaratnam 1990, Chanson 2001). The friction factor on a stepped spillway is quantified as the average shear stress in the air-water flow region downstream of the inception point. In the present study, no uniform equilibrium flow was achieved along the stepped chutes. Therefore the Darcy friction factor was calculated to quantify the average shear stress in the gradually-varied flow for the flat and pooled stepped spillways in the present study (Chanson et al. 2002):

$$f_e = \frac{8 \times \tau_o}{\rho_w \times U_w^{\ 2}} = \frac{8 \times g \times S_f \times d}{U_w^{\ 2}} \tag{9}$$

where the friction slope equals $S_f = -\,\partial H/\partial x$, H is the total head and x is the distance in flow direction.

The experimental results for the flat and (porous) pooled stepped spillways are summarised in Figure 9, in which the friction factor is plotted as a function of the dimensionless step roughness height k_s/D_H with D_H the equivalent pipe diameter. Figure 9 includes all transition and skimming flow data for the flat and pooled step configurations. The data are compared with the solution of a simplified analytical mixing length model, which expressed the pseudo-boundary shear stress $f_d = 2\times\pi^{0.5}/K$, where f_d is an equivalent Darcy friction factor estimate of the form drag and $1/K$ represents the dimensionless rate of expansion of the shear layer (Chanson 2001).

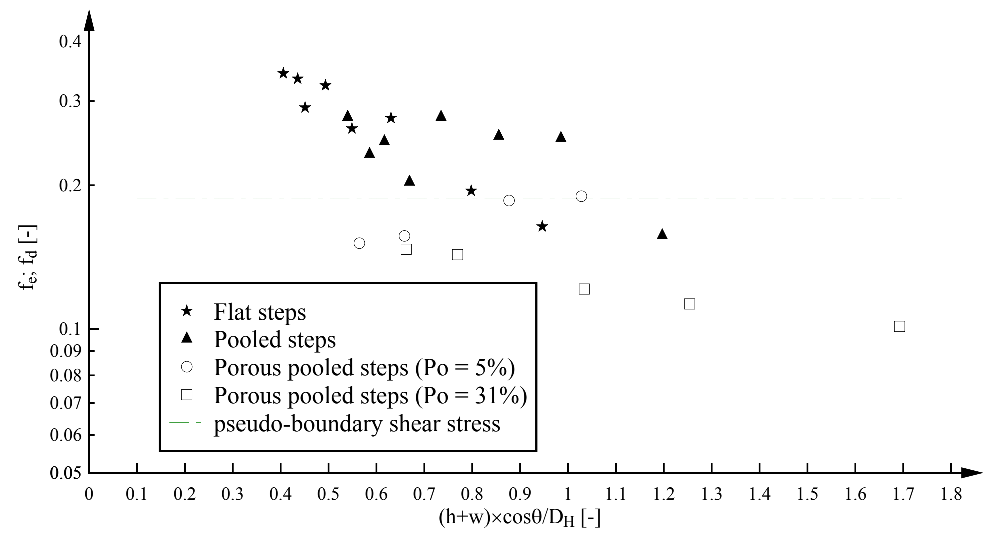

Figure 9. Comparison of Darcy friction factors on the stepped spillways with flat, pooled and porous pooled steps; Comparison with pseudo-boundary shear stress

Overall the stepped spillway data yielded Darcy-Weisbach friction factors between 0.1 and 0.34 (Figure 9). The findings were consistent with the reanalyses of flow resistance data showing variations of Darcy friction factors between 0.1 and 0.35 for $\theta = 15.9°$ and $\theta = 21.8°$ (Felder & Chanson 2009). For the present data ($\theta = 26.6°$), the smallest values of f_e were observed for the porous pooled steps which confirmed the reduction of form drag and momentum exchange by the pores.

6 CONCLUSION

A physical study was conducted on a relatively large stepped spillway with $\theta = 26.6°$ comprising four configurations with flat, pooled and porous pooled steps. The flow patterns showed a close agreement between the nappe, transition and skimming flow regimes for the flat and pooled stepped spillways. However, some small instabilities were observed for the pooled stepped spillway in nappe flows which was linked with pulsating flows in the first pool. The porous pooled stepped spillways showed similar flow patterns in the main stream flow, but some small differences were observed in the pool cavity region. Some discharge appeared through the pores, and decreased the cavity recirculations and air entrainment into the porous pooled step niche. The comparison of the air-water flow properties for the flat, pooled and porous pooled stepped spillways was conducted for transition and skimming flows. The comparative analyses showed a good agreement in most air-water flow property distributions including the void fraction and dimensionless interfacial velocity V/V_{90}. However, the pooled and porous pooled stepped spillways exhibited some larger interfacial velocities V/V_c for all flow rates, a result which was counter-intuitive. However, the comparison of the residual energy at the downstream end showed a smaller energy dissipation rate for the (porous) pooled stepped spillways. The pores decreased the momentum exchange between cavity recirculation and main stream flow and decreased the form drag which resulted in smaller friction factors.

The present testing provided some valuable design implications. The pooled step design showed some pulsating flow patterns for small flow rates which led to some small instabilities. The energy dissipation rate was smaller compared to the flat stepped design performances. The introduction of porosity to the pooled weir wall eliminated any flow pulsations and the flow patterns were stable for all flow discharges. However, the energy dissipation rate was much smaller compared to the flat and pooled step configurations. In summary the porous pooled step design was preferable to the pooled stepped design because the flow was more stable. The practical use of porous pooled steps in prototype requires some thorough physical modeling to ensure that the energy dissipation rate is accurately quantified. The porous pooled stepped spillway with Po = 31% had a porosity comparable to gabions, and the aeration and energy dissipation performance on hydraulic structures with gabion technique should be investigated before any implementation in a prototype environment.

7 ACKNOWLEDGEMENTS

The authors thank Jason Van Der Gevel and Stewart Matthews for their technical assistance. The financial supports through a UQ research scholarship and through the Australian Research Council (Grant DP120100481) are acknowledged.

NOTATION

C	void fraction or air content
C_{mean}	mean air concentration
D_H	hydraulic diameter
d	equivalent clear water flow depth
d_c	critical flow depth
F	bubble count rate
f_d	Darcy friction factor estimated of the form drag
f_e	equivalent Darcy friction factor
g	gravity acceleration constant
H	total head
H_{res}	residual energy
h	step height
K	expansion rate of shear layer
l	step length
N	power law exponent

Po	porosity of porous pooled steps
q_w	water discharge per unit width
S_f	friction slope
U_{Po}	flow velocity through pores
U_w	mean flow velocity
V	interfacial velocity
V_c	critical flow velocity
V_{90}	interfacial velocity where C = 90%
W	channel width
w	pool weir height
x	distance in flow direction
Y_{90}	characteristic flow depth where C = 90%
y	direction normal to the pseudo-bottom formed by the step edges
z	transverse direction
$Ø$	diameter of pores and probe tips
ΔH	energy difference between the two sides of the porous wall
Δx	longitudinal separation between probe tips
Δz	transverse separation between probe tips
ζ	resistance coefficient
θ	channel slope
τ	shear stress

REFERENCES

Abdul-Khader, M.H., Rai, S.P. (1980). A Study of Channel obstructions with a Longitudinal Slot. - Proc. 7th Australasian Hydraulics and Fluid Mechanics Conf., IEAust., Brisbane, Australia, pp. 175-178.

André, S. (2004). High velocity aerated flows on stepped chutes with macro-roughness elements., Ph.D. thesis, Laboratoire de Constructions Hydrauliics (LCH), EPFL, Lausanne, Switzerland, 272 pages.

Bung, D.B. (2011). Developing flow in skimming flow regime on embankment stepped spillways., Journal of Hydraulic Research, Vol. 49, Issue 5, pp. 639-648.

Chanson, H. (2001). The Hydraulics of Stepped Chutes and Spillways., Balkema, Lisse, The Netherlands, 418 pages.

Chanson, H., Toombes, L. (2002). Air-Water Flows down Stepped chutes: Turbulence and Flow Structure Observations., Intl Jl of Multiphase Flow, Vol. 28, No. 11, pp. 1737-1761.

Chanson, H., Yasuda, Y., Ohtsu, I. (2002). Flow Resistance in Skimming Flows and its Modelling., Canadian Journal of Civil Engineering, Vol. 29, No. 6, pp. 809-819.

Felder, S., Chanson, H. (2009). Energy dissipation, flow resistance and gas-liquid interfacial area in skimming flows on moderate-slope stepped spillways., Environmental Fluid Mechanics, Vol. 9, No. 4, pp. 427-441.

Felder, S., Chanson, H. (2011). Energy Dissipation down a Stepped Spillway with Non-Uniform Step Heights., J. of Hydraulic Eng., ASCE, Vol. 137, No. 11, pp. 1543-1548.

Felder, S., Chanson, H. (2012). Air-Water Flow Measurements in Instationary Free-Surface Flows: a Triple Decomposition Technique., Hydraulic Model Report No. CH85/12, School of Civil Engineering, The University of Queensland, Brisbane, Australia, 161 pages.

Felder, S., Guenther, P., Chanson, H. (2012). Air-water flow properties and energy dissipation on stepped spillways: a physical study of several pooled stepped configurations., Hydraulic Model Report No. CH87/12, School of Civil Engineering, The University of Queensland, Brisbane, Australia, 225 pages.

Gonzalez, C.A., Chanson, H. (2007). Hydraulic Design of Stepped Spillways and Downstream Energy Dissipators for Embankment Dams., Dam Engineering, Vol. 17, No. 4, pp. 223-244.

Gonzalez, C.A., Chanson, H. (2008). Turbulence and cavity recirculation in air-water skimming flows on a stepped spillway., Journal of Hydraulic Research, Vol. 46, No. 1, pp. 65-72.

Kökpinar, M.A. (2004). Flow over a Stepped Chute with and without Macro-Roughness Elements., Can. Jl of Civil Engineering, Vol. 31, No. 5, pp. 880-891.

Meireles, I., Matos, J. (2009). Skimming Flow in the Nonaerated Region of Stepped Spillways over Embankment Dams., J. of Hydraulic Eng.- ASCE, Vol. 135, No. 8, pp. 685-689.

Naudascher, E., Rockwell, D. (1994). Flow-Induced Vibrations. An Engineering Guide. - IAHR Hydraulic Structures Design Manual No. 7, Hydraulic Design Considerations, Balkema Publ., Rotterdam, The Netherlands, 413 pages.

Ohtsu, I., Yasuda, Y., Takahashi, M. (2004). Flow Characteristics of Skimming Flows in Stepped Channels., Jl of Hydraulic Eng., ASCE, Vol. 130, No. 9, pp. 860-869.

Peyras, L., Royet, P., Degouette, G. (1992). Flow and Energy Dissipation over Stepped Gabion Weirs., J of Hydraulic Eng., ASCE, Vol. 118, No. 5, pp. 707-717.

Rajaratnam, N. (1990). Skimming Flow in Stepped Spillways., Jl of Hydraulic Eng., ASCE, Vol. 116, No. 4, pp. 587-591.

Relvas, T.R., Pinheiro, A.N. (2008). Inception Point and Air Concentration in Flows on Stepped Chutes lined with Wedge-shaped Concrete Blocks., J. of Hydraulic Eng., ASCE, Vol. 134, No.8, pp. 1042-1051.

Saryanarayana, G.K., Pauer, H., Meier, G.E.A. (1993). Bluff-Body Drag Reduction by Passive Ventilation., Experiments in Fluids, Vol. 16, No. 2, pp. 73-81.

Thorwarth, J. (2008). Hydraulisches Verhalten der Treppengerinne mit eingetieften Stufen – Selbstinduzierte Abflussinstationaritäten und Energiedissipation. (Hydraulics of Pooled Stepped Spillways – Self-induced Unsteady Flow and Energy Dissipation.); Ph.D. thesis, University of Aachen, Germany (in German).

Thorwarth, J., Köngeter, J. (2006). Physical Model Test on a Stepped Chute with Pooled Steps – Investigation of Flow Resistance and Flow Instabilities. - International symposium on Hydraulic Structures, Caracas, Venezuela:, pp. 477 – 486.
Tsukahara, T., Sakamoto, Y., Aoshima, D., Yamamoto, M., Kawaguchi, Y. (2012). Visualisation and laser measurements on the flow field and sand movement on sand dunes with porous fences., Experiments in Fluids, Vol. 52, No. 4, pp. 877-890.